FERMILAB-CONF-12-647-APC

DIELECTRIC-PLATE-IMPLANTED HIGHER ORDER MODE (HOM) WAVEGUIDE FOR HIGH INTENSITY MULTI-BEAM DEVICE APPLICATION

Young-Min Shin, Department of Physics, Northern Illinois University, Dekalb, IL 60115, USA
Accelerator Physics Center (APC), FNAL, Batavia, IL 60510, USA

Abstract

A mode-selective oversized RF-beam channel has been investigated for high intensity multi-beam devices. Implanting the equi-spaced dielectric plates at the transverse positions where longitudinal electric fields of a HOM are minimal in the micro-metallic structure strongly suppresses all lower energy modes and other wakefield modes. The dielectric lattice captures only a single HOM of the wavelengths that correspond to the plate spacing. Electromagnetic simulations have shown that the lower energy modes, TE_{10} and TE_{20} modes, are suppressed down to < ~ - 60 dB by two plate loads, while TE_{310}-mode prominently propagates through the 2 mm long waveguide only with – 4 dB (= - 2dB/mm) at 1 THz. The numerical calculation indicated that the TE_{30} mode has ~ a few times higher Q than the lower energy modes. The strong single mode selectivity has been extensively looked into with a more highly overmoded structure. Feasibility analysis of the HOM structure for multi-beam device application is under investigation. Particle-in-cell (PIC) simulation has shown coherent beam bunching and energy gain from THz driving signal. Multi-beam RF interaction could be an attractive scheme to resolve instability issues in the low energy region.

INTRODUCTION

There have been continuous demands for multi-beam interaction scheme in the accelerator and RF source community as cooling high brightness beams is one of the most challenging issues for intense beam devices [1 - 4]. To obtain high intensity ion beams from an accelerator stably, it is necessary to suppress the defocusing force due to the space charge effect. This divergent force is proportional to the beam current and to the inverse square of the beam velocity. Splitting the beam current into smaller segments is one of the promising approaches to mitigating the diverging space charge force of high brightness beams. For the same reason, multi-beam can also deliver more beam power to a RF cavity if individual beam current remains consistent over the beams. In order to utilize maximum field interaction from multi-beam system, a RF structure must be designed with HOM configuration. The critical disadvantage of HOM-operation is that over-moded structures have severe mode-competition that would possibly cause excitation and amplification of trapped wakefields. The disturbed beam collimation can induce a beam breakup.

Quasi-optical electromagnetic crystal structures [5, 6] have been developed for multi-beam devices to effectively segregate an operating HOM from competing noise modes and efficiently damp trapped wakefields. This paper will present the novel HOM accelerating structure, which is designed with laterally arrayed dielectric-plates in the staggered double grating micro-channel. This EM crystal mode filter is a periodic of materials that attenuate EM waves of certain cavity- or waveguide-modes from propagating through. These quasi-optical resonators offer many advantages over conventional pillbox cavities and oversized waveguides by suppressing the non-operating modes in the RF structures [7].

DISPERSION AND SIGNAL RESPONSE ANALYSIS

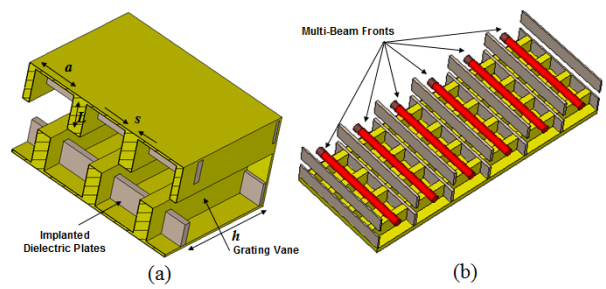

Figure 1: (a) HOM travelling waveguide implanted with dielectric-plate lattices (b) conceptual drawing of high intensity multi-beam device with EM crystal damper.

The multi-beam HOM accelerating structure was designed with the oversized rectangular waveguide that is corrugated with two metal gratings. The axial position of two gratings is half-period-staggered to impose axial electric field components on the interactive passbands. The thin lossy dielectric plates are implanted in the gratings along the circuit axis. Figure 1(a) shows a conceptual drawing of the proposed structure. In the structure, as the lattices are placed at the field minimum positions of an operating mode, the presence of the lossy rods leads to nearly zero perturbation of the field distribution. However, non-resonant modes experience severe attenuation due to high-field absorption of dielectric ohmic losses. Figure 1(b) shows a schematic of a high-intensity beam HOM device in the multi-cell metallic micro-channel. Depending upon beam emitter type, the beam shape can have a cylindrical, elliptical, or rectangular configuration.

Copyright © 2012 by IEEE – cc Creative Commons Attribution 3.0 (CC BY 3.0) — cc Creative Commons Attribution 3.0 (CC BY 3.0)

ISBN 978-3-95450-115-1
Operated by Fermi Research Alliance, LLC under Contract No. De-AC02-07CH11359 with the United States Department of Energy.

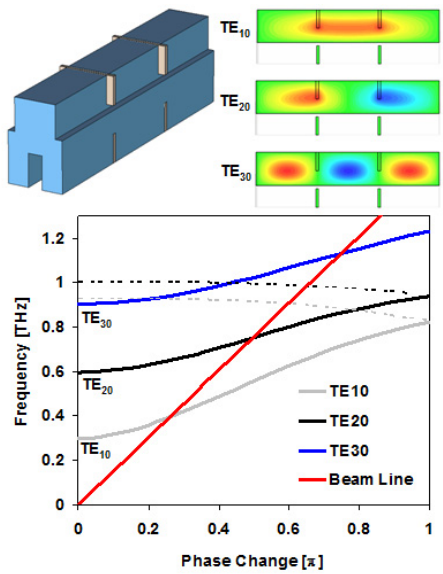

Figure 2: Dispersion curves and electric field plots (E_z) of three accelerating modes (TE_{10}, TE_{20}, and TE_{30}) (the dotted lines denote backward wave modes).

For simple simulation analysis, a three-beam micro-structure is first designed with two dielectric rods, which are defined by Aluminum Nitride ($\varepsilon = 20$, $\delta_t = 0.25$) in the copper waveguide ($\sigma = 5.8 \times 10^7\ \Omega^{-1}m^{-1}$). In order to manifest the effect of loading the optical defects, the structure size has been designed at the 1 THz range where it is heavily affected by absorption losses. Figure 2 shows longitudinal field plots and dispersion graphs of the first three waveguide modes (TE_{10}, TE_{20}, and TE_{30}). For f (TE_{30}) = 1.02 THz, normalized geometrical dimensions of the designed structure are given as follows: $L = 0.27\ \lambda$, $a = 0.345\ \lambda$, $d = 0.46\ \lambda$, $b = 0.15\ \lambda$, and $h = 0.77\ \lambda$. Figure 2(b) shows dispersion graphs of the three waveguide modes, calculated from CST-MWS eigenmode solver. One can see that the relativistic beam passes over lower energy modes (f (TE_{10}) = 0.4 THz and f (TE_{20}) = 0.75 THz) on the two fundamental passbands. It also meets with two backward wave modes (dotted lines) of 2nd higher TE_{10} and TE_{20} bands. The over-moded beam-wave coupling can trap parasite wakefields in the beam tunnel, dispersing the beam energy over a wide spectrum. As shown in the field plot (top-right), the rods, though, intensively distort the field distributions of the two most dominant lower modes, while one of the TE_{30} modes (designed operating mode) shows no change with the lossy dielectrics. The two equi-spaced ohmic rods impose huge energy absorption to two non-resonating modes.

Figure 3 shows transmission graphs (S_{21}) of the 2mm-long channels (20 longitudinal cells) without the dielectric rods, (a), and with the ones, (b). In Fig. 3(a), the three modes have nearly the same amount of insertion losses, ~ - 0.45 dB (= ~ 0.225 dB/mm, TE_{10}), ~ - 1 dB (= ~ 0.5 dB/mm, TE_{20}), and ~ -1.2 dB (= ~ 0.6 dB/mm). Over the frequency range, ~ 1 THz, where these three passbands are heavily overlapped, the three accelerating modes are thus strongly competing. However, the transmission graph of the dielectric-loaded waveguide in Fig. 3(b) clearly shows that the two lower modes are noticeably suppressed down to ~ - 60 dB (= ~ 300 dB/mm, TE_{10}) and ~ - 80 dB (= ~ 400 dB/mm, TE_{20}). On the other hand, the TE_{30} mode still remains consistent with the same transmission loss, ~ - 3dB (= ~ 1.5 dB/mm). Adding the lossy material in the structure somewhat reduces field intensity, but this strong mode suppression allows only a single HOM to mono-energetically couple with electrons, equally distributing EM energies over the beams.

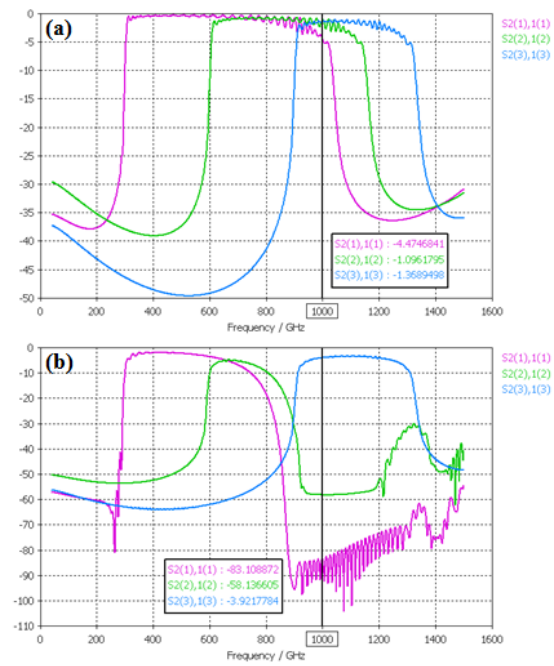

Figure 3: Transmission graphs of three accelerating modes (TE_{10}, TE_{20}, and TE_{30}) with (a) typical over-moded corrugated waveguide and (b) dielectric-loaded one.

PARAMETRIC ANALYSIS

The R/Q and Q of the designed structure have been calculated for three accelerating modes (two low energy modes: TE_{10} and TE_{20}, and one resonating mode: TE_{30}) in terms of frequency. From the eigenmode solver simulations, R/Qs were calculated at the transverse position of the maximum electric fields. In Fig. 4(a), two lower frequency modes have more or less higher interaction impedances (TE_{10}: = 12 ~ 16 Ω and TE_{20} = 7.6 ~ 12.6 Ω) than the TE_{30} one over the passbands (= 5.3 ~ 12.6 Ω). However, as shown in Fig. 4(b), the ohmic Q (Q_0) = 200 ~ 450) of TE_{30} overwhelms the ones (TE_{10} = 20 ~ 40 and TE_{20} = 25 ~ 60) of the others in the 1 THz range. This numerical analysis on the circuit parameters more quantitatively depicts that the lossy rods selectively attenuate non-resonating wakefields by strong evanescent absorption of off-standing waves. More systematic analytical and experimental examinations on structural characteristics are under way.

Copyright © 2012 by IEEE – cc Creative Commons Attribution 3.0 (CC BY 3.0) — cc Creative Commons Attribution 3.0 (CC BY 3.0)

PARTICLE-IN-CELL MODELING

This novel RF accelerating structure has been simulated with three electron beams that are modeled with the rectangular configuration (~ 67% and ~ 90% tunnel-filing factors in minor and major axes, respectively). In order to observe a beam bunching within a practical simulation time scale of the THz range, the beam energy is set to be in a non-relativistic level (~ 20 keV and ~ 0.25 A), which is designed to be synchronized with the driving signal (f_{TE30} = 1 THz, P = 1 Watt) of the 1st spatial harmonic (n = 1). Figure 5 very clearly shows that each of the fully bunched beams has 180-degree phase difference with the others. The spatial energy distribution is correspondingly matched with the field pattern of TE_{30}. Figure 5(b) shows frequency spectrum of RF signals obtained from the bunched beams at the end of the computational model: TE_{30} signal appears more noiseless and ~ 20 and ~ 30 dB stronger than TE_{10} and TE_{20} ones. The PIC simulation result supports that implanting an optical lattice load absorbs the non-resonating fields so strongly as to have no interaction with the electron beams. The mode filtering scheme is very simple and suitable for any type of multi-beam devices.

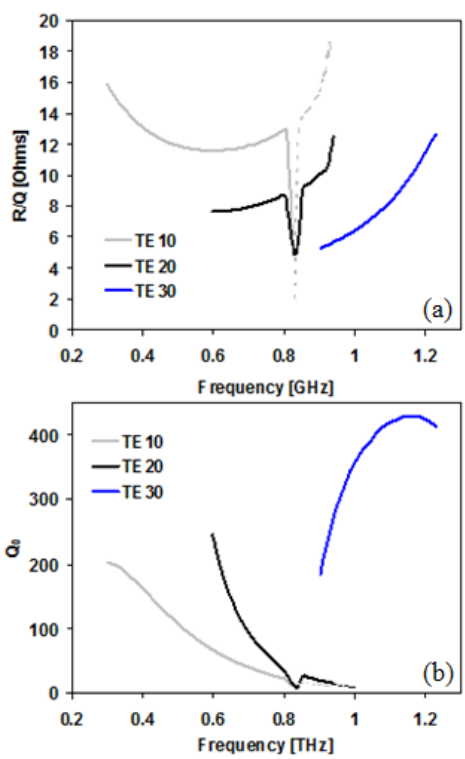

Figure 4: Frequency versus (a) R/Q and (b) Q graphs of three accelerating modes (TE_{10}, TE_{20}, and TE_{30}), calculated from RF simulations.

CONCLUSION

Consequently, a HOM accelerating structure is proposed for a multi-beam type linear accelerator that is a practical and efficient method to accelerate high intensity ion beams. The corrugated waveguide with the dielectric-plate lattice array is simple and power-efficient for low energy region beam accelerations or THz power radiation sources manageable in terms of the alignment of the electrodes.

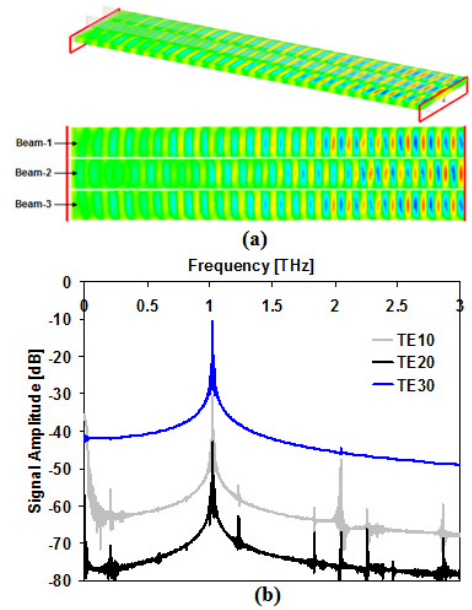

Figure 5: (a) Spatial energy distribution of three modulated electron beam, simulated by 3D particle-in-cell code (CST-PIC solver) (b) frequency spectra FFTed from time-signals of bunched beams.

REFERENCES

[1] V. Vogel, S. Choroba, et al., "Testing of 10MW Multibeam Klystrons for the European X-Ray FEL at DESY", Proc. of PAC07, Albuquerque, New Mexico, USA, pp. 2077. (2007).

[2] E. Jesen, "Development and Future Prospects of RF Sources for Linac Applications", 25th Linear Accelerator Conference, Tsukuba, Japan, 12 - 17 Sep 2010, pp. TH103.

[3] Takuya Ishibashi, Noriyosu Hayashizaki, Toshiyuki Hattori, Taku Ito, Liang Lu, and Jun Tamura, "Multibeam cavity for low energy beam acceleration", Nuclear Instruments and Methods in Physics Research B 261 13−16 (2007).

[4] A. V. Mishin, R. Schonberg, H. Deruyter, T. Roumbanis, R. Miller, J. Potter, "Multiple Beam Coupled Cavity Microwave Periodic Structure", International Linear Accelerator Conference, Geneva, Switzerland, 26 - 30 Aug 1996, pp. 809-811.

[5] A. Smimov, D. Newsham, D. Yu, "PBG cavities for single-beam and multi-beam electron devices", Proceedings of the 2003 Particle Accelerator Conference, 1153 (2003).

[6] D. Newsham, A. Smirnov, and D. Yu, "Multi-Beam Photonic Band Gap Structure", Infrared and Millimeter Waves, 2002. Conference Digest, Twenty Seventh International Conference on , 109 – 110 (2002).

[7] E.N. Comfoltey et al., "Design of an overmoded W-band TWT" Vacuum Electronics Conference (IVEC '09). IEEE International, 127-128 (2009).

Copyright © 2012 by IEEE – cc Creative Commons Attribution 3.0 (CC BY 3.0) — cc Creative Commons Attribution 3.0 (CC BY 3.0)

ISBN 978-3-95450-115-1